

## THERMAL BUCKLING OF STUD SUPPORTED LINER SHELLS

Th.P. KICHER, Th.C. ESSELMAN, R.J. GRATZINGER

*Solid Mechanics, Structures and Mechanical Design Division, School of Engineering  
Case Western Reserve University, Cleveland, Ohio 44106, U.S.A.*

### SUMMARY

The buckling and post buckled behavior of liner shells for concrete containment vessels have been examined both analytically and experimentally. Earlier work of the authors is extended to include the effects of biaxial loading and anchor flexibilities. This analysis method is based on the theories of minimum potential energy and an assumed displacement state. First a displacement pattern representing the experimentally observed out-of-plane displacement is determined. The associated membrane displacements are determined from the nonlinear equilibrium equations for cylindrical shells. Then the total displacement state is used to generate a potential energy function. The minima of this function are the equilibrium positions. The pre and post buckling response of the system are obtained by numerical solution and buckling is defined using Tsien's lower bound criteria. Using this basic analysis scheme, two major tasks on the buckling of liner shells are reported.

An analysis for complete cylindrical shell elements anchored with rigid studs and subjected to biaxial loads is presented. A displacement state which satisfies two zero slopes and a zero displacement at the studs is assumed. Several distinct modes of buckling were found and the critical mode identified. Experiments on models of complete cylindrical shells subjected to thermal loading are summarized and correlated with analytical predictions. Design charts for determining rectangular stud spacings for various combinations of biaxial load are obtained from this study.

A one-dimensional beam model for liner shells with flexible anchors is also presented. A displacement pattern for a segment of a liner supported by elastic studs is assumed. Stud stiffness properties were obtained by a simple stress analysis model and confirmed by experimental data from the literature. Liner and stud loads before and after buckling were predicted from the assumed displacement pattern. Combinations of mechanical and thermal loading were used to determine the buckling loads experimentally. The effects of anchor flexibilities on the buckling loads and the anchor loads after buckling were measured experimentally. Design charts for estimating stud sizes to support a buckled panel are obtained from this study.

## 1. INTRODUCTION

When concrete tanks are used as containment or pressure vessels they must be lined to assure a leak tight seal. Generally a steel shell is used as a liner and is anchored to the concrete with continuous ribs or point anchors. The liners are subjected to both mechanical and thermal loads. These may occur as a result of normal operating conditions or as the result of an accident. The criteria of failure for the vessel elements i.e. liner, anchors and concrete depend on the loading condition. For example, stresses (strains) in the liner in excess of a buckling criteria can not be tolerated for the loads associated with normal operating conditions. At the same time, buckling of a liner can be tolerated during an accident so long as the liner continues to function as a leak tight seal.

The problem of the buckling of an unsupported ring encased in a rigid cavity was first examined by Lo, Bogdanoff, Goldberg and Crawford [1]. The ring was subjected to a temperature rise  $\Delta T$  resulting in a compressive stress due to the constraint of the rigid cavity. The ring snaps into an elliptic sine wave about the cord line connecting tangency points. The Tsien [2] equal energy criteria was used to define the buckling load since this system does not exhibit a bifurcation point. Chan and McMinn [3,4] found approximate solutions to the problem of the constrained buckling of a ring and ring segments using a circular sine function as an assumed displacement shape. Subsequently they determined the length of ring segments (anchor spacing) for which buckling would be suppressed. This work was verified by a series of tests on ring segments which remained elastic throughout the pre and post buckling response. Because of the completely elastic behavior, buckling was identified by the load level at which the ring returned to an unbuckled shape.

Hsu, Elkou and Pian [5] found that geometric imperfections of the ring shape introduced a bifurcation point but did not substantially alter the post buckling response. Bucciarelli and Pian [6] examined the effects of placing a ring into a geometrically imperfect cavity. Three subcases of response phenomena were observed and related to the sign of the curvature of the initial imperfections: (a) for imperfections with negative curvatures everywhere, no bifurcation point exists; (b) for imperfections with zero slope and curvature over a finite span (flat spot) with the remaining curvature being negative, the system has a bifurcation point and snap buckling may occur; (c) for imperfections, with both positive and negative curvatures a maximum point is observed in the response curve.

Zagustin and Herrmann [7] studied the problem of the snap buckling confined ring subjected to a uniformly distributed parallel loading in the plane of the ring. This solution is essentially a static treatment of the inertial load problem, also examined by Pian and Bucciarelli [8].

Chicurel [9] examined the confined ring using a circular sine function as an assumed displacement mode and examined two cases: no-slip and no-friction. The results were compared with those presented in Reference [1].

More recently Burgess [10] studied a radially constrained imperfect circular ring using a shallow beam model. A piecewise continuous solution and a discrete element solution are shown to converge as the number of elements is increased. El-Bayoumy [11] also studied the radially constrained circular ring using a shallow arch approximation. These results also indicate a snap phenomena buckling with the magnitude of the energy barrier decreasing with increased loading.

Allan [12,13] examined the problem of a flat strip subjected to an axial thrust and confined by a rigid constraint on one side. The other side of the strip was subjected to a dead weight load [12] or an elastic foundation loading [13]. Both solutions exhibit large displacement post buckling equilibrium positions with the elastically restrained column supporting a larger load than the column with the dead weight lateral load. Anderson [14] examined the buckling of a strip on a geometrically imperfect rigid support and subjected to normal pressure. A similar problem of the buckling of a finite length simply supported beam between two unattached elastic foundations was examined by Burkhard and Young [15].

A series of four papers [16,17,18,19] presented at the Institution of Civil Engineers Conference on Prestressed Concrete Pressure Vessels focused on the analysis, design and construction of liners and anchors. This series of papers provides a good survey of the problems associated with the proper specification of liners and anchors. However none of these papers dealt with the complications of shell behavior in studying the buckling and post buckling response. All of the stress analysis models are based on either an elastic strip or rigid link-plastic hinge model and ignored any post buckling response of the liner. These papers do present experimental data which supports the validity of the models presented.

Substantially fewer investigators have directed their attention to the buckling of two dimensional plate and shell elements which are constrained and subjected to thermal and mechanically compressive loads. Doyle and Chu [20] analyzed the anchor loads in plate liner elements where the buckling load is exceeded. Kiesling, DeHart, and Jain [21,22] presented the results of an extensive investigation on the buckling of ring stiffened cylindrical shells encased in concrete subjected to external pressure. Several alternate failure modes were observed experimentally: panel buckling, stiffener yield and shell tearing. This study resulted in a design procedure for the tunnel liners in the California State Water Project.

Kicher [23] presented an assumed mode solution for the buckling of stud supported thin cylindrical liner shells encased in concrete. Two modes of buckling were examined: displacements uniform in the axial direction (ring mode) and displacements uniform in the circumferential direction (axisymmetric mode). A buckling mode resulting from the superposition of these two mode shapes was suggested but was not treated.

Finally, Tong and Pian [24] presented solutions for the radially constrained spherical shell subjected to axisymmetric edge loading using both deep shell and shallow shell models. The effects of initial imperfections were included in the shallow shell model.

This review of the literature indicated the need for an analysis of the buckling and post buckling behavior of stud supported cylindrically shaped liner shells encased in concrete. Furthermore there was a lack of experimental data on the buckling loads and anchor loads after buckling. These data were needed for correlation with and verification of the analysis as well as setting design criteria for selecting the liners and anchors. An accurate buckling prediction is needed so that the design will not suffer excessive displacements due to buckling during normal operating conditions. The predictions of liner stresses and anchor loads during and after buckling is needed to guarantee the integrity of the liner in the event of an accident.

The work of Kicher [23] was expanded and a two dimensional buckling pattern was examined for the case of rigid studs. This same analysis method was used to treat a ring supported by elastic studs and encased in concrete. This paper summarizes the results of these studies. The reader is referred to references [25] and [26] for further details of these studies.



C - Region where liner detaches in a strip mode

D - Region where liner remains in a membrane state in contact with the cavity

Using the homogeneous and particular solutions, displacement states for the individual regions can be established. Next the requirements of continuity of displacements and bending slopes is imposed to obtain the following displacement patterns.

Region A - Intersection of Ring and Strip Modes

$$W = A_0(1 - \cos nR\theta) + A_x(1 - \cos mx) \quad (2)$$

$$u = \frac{xH}{a}(a - l_x) + x\epsilon_x + \frac{vA}{mR} \sin mx + \frac{m}{8} A_x^2 \sin 2mx + \frac{mn^2(n^2 - vn^2)}{(m^2 + n^2)^2} A_x A_0 \sin mx \cos nR\theta \quad (3)$$

$$v = \frac{\theta J}{\theta_0}(\theta_0 - \theta_p) + R\theta\epsilon_\theta + \frac{A_0}{nR} \sin nR\theta + \frac{n}{8} A_0^2 \sin 2n\theta + \frac{m^2 n(m^2 - vn^2)}{(m^2 + n^2)^2} A_x A_0 \cos mx \sin nR\theta \quad (4)$$

Region B - Ring Mode

$$W = A_0(1 - \cos nR\theta) \quad u = H(x - l_x) + x \epsilon_x \quad (5,6)$$

$$v = \frac{\theta J}{\theta_0}(\theta_0 - \theta_p) + R\theta\epsilon_\theta + \frac{A_0}{nR} \sin nR\theta + \frac{n}{8} A_0^2 \sin 2n\theta \quad (7)$$

Region C - Strip Mode

$$W = A_x(1 - \cos mx) \quad u = \frac{xH}{a}(a - l_x) + x\epsilon_x + \frac{vA}{mR} \sin mx + \frac{m}{8} A_x^2 \sin 2mx \quad (8,9)$$

$$v = J(\theta - \theta_p) + R\theta\epsilon_\theta \quad (10)$$

Region D - Membrane

$$W = 0 \quad u = H(x - l_x) + x\epsilon_x \quad v = J(\theta - \theta_p) + R\theta\epsilon_\theta \quad 11,12,13$$

where H and J are unknown membrane displacement magnitudes and  $\epsilon_x$  and  $\epsilon_\theta$  are the imposed membrane strains

The total potential energy becomes a function of all of the unknown displacement magnitudes  $A_x$ ,  $A_0$ , H and J and the lengths of the detached regions a and  $\theta_0$ .

$$\pi = \pi(A_x, A_0, H, J, a, \theta_0) \quad (14)$$

The stationary conditions on the total potential energy leading to the conditions for equilibrium are that all of the first partial derivatives of the total potential energy with respect to the independent variables must vanish simultaneously. These conditions lead to six simultaneous nonlinear algebraic equations which have unique multiple solutions. The solution procedures used for these equations are extremely complicated and required the use of a digital computer. The details of the solution method are not presented here: the reader is referred to reference [25] for the complete discussion.

In summary, nine types of solutions were observed representing the various combinations of pure membrane, ring mode, strip mode and the intersection of the ring and strip mode which span only part or all of the liner element between studs. Figure 2 is a graphical presentation of the various types of solutions based on the extent of the propagation of the buckle and detached region between stud supports. If the applied strains are imposed in a fixed ratio  $\beta = \epsilon_x/\epsilon_\theta$  the solutions to the buckling response appear to lie along a line which starts from the upper left of Figure 2 ( $\theta_0/\theta_p = 0$  and  $a/l_x = 0$ ) and drops diagonally to the lower right. The slope of this line is a function of  $\beta$  while the location of the solution along

this line depends on the strain magnitude. Figure 3 is a plot of the post buckling response curves for various load ratios applied to a liner supported with a square array of studs and one case of a rectangular array of studs. Sets of curves of this type were generated for each of the numerical examples. If the liners and anchors are designed so that buckling is precluded, Tsien's [28] lower bound criteria sets the buckling strain at the minimum post buckling strain. Figures 5, 6 and 7 are the minimum post buckling strains for shells with  $R/t = 2000$  subjected to various states of combined strain  $\beta = 0, 0.5$  and  $1.0$  as functions of stud spacings. The solid lines represent a buckle mode composed of the interaction of both the ring and strip modes. The broken line represents buckling in a mode composed only of the ring mode. The curves are composed of two distinct segments, a hyperbolically shaped portion to the left and a horizontal asymptote to the right. The entire family of buckling curves for various longitudinal stud spacings is contained within a lower bound envelope for the ring. This simple observation has extremely far reaching consequences. Within the limits of this study this observation can be summarized in the following way: for a rectangular array of studs, the circumferential spacing of studs controls the strain at which the liner will buckle. The minimum buckling strain is independent of the longitudinal spacing of the studs.

The longitudinal spacing of the studs will enter the design procedure through the requirement that sufficient studs should be available at the end of the fully propagated ring mode to arrest the buckle wave. Furthermore it is necessary to know the magnitude of the forces in a buckled liner and the load carried by the studs adjacent to the buckle in the liner. Such data cannot be obtained from this analysis since the studs were assumed to be rigid rendering the forces indeterminable. This leads to the second model studied under this investigation.

#### 4. FLAT PLATE AND RING MODELS

Consider a circumferential slice from a lined concrete shell. If all axial variation effects are ignored, this model can be used to study the behavior of a liner shell supported by elastic studs. Each stud is assumed to have three degrees of elastic freedom; extension, shear and flexure as shown in Figure 7. If these deformations of stud supports are permitted, additional degrees of freedom will be introduced into the liner behavior. The buckling of a liner shell will be dominated by separation in one span between studs. The regions of the liner immediately adjacent to the buckle will be separated from the cavity but only due to the extension and flexure freedom of the stud. All other regions of the liner will be in contact with the cavity, and will slide introducing a stud shear load which diminishes with increasing distance from the buckle. The point on the liner which is diametrically opposite the maximum buckle will suffer no shear or tangential displacement. Figure 8 is a graphical presentation of this hypothesized buckle pattern. Figure 9 shows the terms of the transverse displacement pattern. The corresponding membrane displacement is determined by solving the nonlinear membrane equilibrium equations. The shear flexibility of the studs is reflected in the liner by allowing tangential displacements at each stud through the homogeneous portion of the solution. Using the regions identified in Figure 8 the following assumed displacement patterns are established.

Region I - Primary Buckle in Liner

$$W = w_0 + w_0' \frac{\theta^2}{\theta_0} + A_0 (1 + \cos nR\theta) \tag{15}$$

$$v = \frac{w_o \theta^3}{3\theta_p} \left(1 + \frac{2w'_o}{R\theta_p}\right) - \frac{A_\theta}{nR} \left(1 - \frac{2w'_o}{R\theta_p}\right) \sin nR\theta - \left(\frac{2w'_o}{R\theta_p}\right) A_\theta \cos nR\theta - \frac{nRA_\theta^2 \theta}{4} + (Q_1 + R\epsilon_\theta)\theta + \left(\frac{nA_\theta^2}{8}\right) \sin 2nR\theta \quad (16)$$

Region II - Adjacent to Buckled Liner

$$W = H_1 \left[2\theta_p^3 - 3\theta_p^3 \left(\theta - \frac{\theta_p}{2}\right) + \left(\theta - \frac{\theta_p}{2}\right)^3\right] - H_2 \left[\left(\theta - \frac{\theta_p}{2}\right)^2 - 2\theta_p \left(\theta - \frac{\theta_p}{2}\right) + \theta_p^2\right] \quad (17)$$

$$v = H_1 \left[\frac{3}{2} \theta_p^2 \theta^2 - \frac{1}{4} \left(\theta - \frac{\theta_p}{2}\right)^4\right] \left(1 - \frac{2H_2}{R}\right) + H_1 \left[\frac{3H_1}{R} \theta_p^2 \left(\theta - \frac{\theta_p}{2}\right)^3 - \frac{9H_1}{10R} \left(\theta - \frac{\theta_p}{2}\right)^5\right] - H_2 \left[\theta_p \theta^2 - \frac{1}{3} \left(\theta - \frac{\theta_p}{2}\right)^3\right] \left(1 - \frac{2H_2}{R}\right) - H_2 \left[\frac{2H_1}{R} \theta_p \left(\theta - \frac{\theta_p}{2}\right)^3 - \frac{H_1}{R} \left(\theta - \frac{\theta_p}{2}\right)^4\right] + (J_1 + R\epsilon_\theta)\theta + J_2 \quad (18)$$

where

$$H_1 = \frac{4w_o + 3w'_o \theta_p}{2\theta_p^3} \quad \text{and} \quad H_2 = \frac{6w_o + \frac{11}{2} w'_o \theta_p}{2\theta_p^2}$$

Region III - Membrane Liner

$$W = 0 \quad v = (K_1 + R\epsilon_\theta)\theta + K_2 \quad (19,20)$$

After the conditions of displacement and bending slope continuity are imposed on the displacements patterns in adjacent regions, the conditions of equilibrium are satisfied by imposing the stationary conditions on the total potential energy. Again the details of the solution method are not presented herein. The reader is referred to Reference [26].

Numerical results are presented for only one liner/anchor design, namely the 1/3 scale model which was examined experimentally. The results are summarized in Figures 10 through 14 with the details of the anchor design presented in the section on experiments. Figure 10 is the post buckling curves for  $R/t = 2000$  for various circumferential stud spacings. Figures 11 and 12 are plots of hoop strain versus anchor tensile and bending stresses respectively. The left portion of the stud tensile stress curve corresponds to the post buckling region while the right side corresponds to the unstable solutions to the buckling response. The right branch of the stud bending stress curve corresponds to the post buckled region. Figure 13 and 14 are plots of the hoop strain versus the shear displacements of the stud adjacent to the buckle and the stud one bay away from the buckle. It is interesting to note that the tensile stresses of the anchors are larger during the transition through the unstable response and they relax after the liner reaches a stable buckled position. The bending stresses in the anchors take on a maximum value when the liner is in the post buckled position. Finally for high membrane prebuckled strains the anchors must undergo a shear displacement directed away from the buckle during the transient. Ultimately the shear displacements relax towards the buckle after the liner reaches a stable post buckled configuration. The magnitudes of the tensile and bending stresses as well as the shear displacements are dependent on the stiffness coefficients selected for this analysis. These results appear to be particularly low and will be discussed in the next section on the Experimental work.

## 5. EXPERIMENTAL PROGRAM

Few investigators have directed their attention to experimental investigations of the buckling of rings or shells confined in a rigid cavity. Ghan and McMinn [3,4] reported on two experiments conducted in thin initially flat strips bent into a circular cavity and

restrained by an end displacement. In one series of experiments, the left portion of the post buckling curve, i.e., the unstable branch was verified by finding the end load necessary for the strip to conform to a given displacement. The right portion or stable branch of the post buckling curve was examined by forcing the ring into a natural post buckled shape and gradually reducing the load. The load at which the ring snaps back into contact with the cavity is the bottom of the post buckling curve. It is important to recognize that all of these experiments were conducted using materials which remain elastic throughout the pre and post buckling response.

Both of the papers by Allan [12,13] contain experimental data offered as support to the buckling analysis of a flat strip. These data are useful in verifying new theories for strip models, since the experimental work is well documented, i.e., material characteristics, post buckling displacements, forces and wave lengths.

Experimental data for the buckling of liner plate elements were reported in all four of the papers [16,17,18,19] presented at the Institution of Civil Engineers Conference on Prestressed Concrete Pressure Vessels in 1968. These papers present results for materials which exceeded the elastic limit as well as rib and stud anchored flat liners. In fact the work of Doyle and Chu [20] utilized this data in support of their analytical work.

The work of Kiesling, DeHart, Jain and Griffith [21,22] included an experimental investigation of six ring-stiffened cylindrical shells (0.25 inch thick by 45 inch I.D. by 15 feet - 7 1/2" long) encased in concrete. Several alternate designs were examined for the ring stiffeners. All of the liner shells exhibited a lobar form of buckling where the waves propagate to the ring stiffeners in the axial direction. In the circumferential directions, the buckle wave could be approximated by the confined ring mode shape. The photographs of the buckled shells suggest two possible assumed modes for a displacement analysis:

Rings which provide a clamped support

Rings which provide a hinged support

$$W = A(1 - \cos \frac{2\pi x}{l})(1 - \cos \frac{2\pi \theta}{\theta_0})$$

$$W = A \sin \frac{\pi x}{l} (1 - \cos \frac{2\pi \theta}{\theta_0}) \quad (21,22)$$

The work of Kiesling, DeHart, Jain and Griffith serves as a standard for both good design and good research.

In order to provide data to substantiate the buckling analysis of stud supported shell element liners, an experimental program was conducted in conjunction with the analytical work. Models of complete liner shells and ring segments were tested to obtain data on buckling loads (strains or temperatures), post buckling stresses and displacements.

Shell Models

Steel (C1008) liner shells (0.016 inches thick by 30 inches in diameter  $D/t = 1875$ ) were encased in concrete and tested by heating the interior with nichrome wire heaters. Two unsupported shells (without anchors), each 30 inches long, were prepared and tested with the longitudinal axis of the specimen in a vertical orientation. A considerable amount of difficulty was encountered in preparing a specimen so thin and deep. One liner specimen was stabilized with air pressure during the placing of concrete. Since the near hydrostatic external pressure of the concrete was reacted by a uniform internal pressure, a nonuniform residual strain state resulted. A second 30 inch long specimen was stabilized by supporting the interior of the liner with a slurry of sand and water. While this sample was substantially better in terms of initial imperfections and residual stresses, all remaining shell models were reduced to a 10 inch length. A total of four, 10 inch long specimens were tested, one

unsupported and three with point anchors on various rectangularly spaced centers (1) 5/8" axially by 2-1/4" circumferentially, (2) 2-1/4" axially by 5/8" circumferentially and (3) 7/8" axially by 7/8" circumferentially. These stud patterns were selected so that various modes of buckle waves could be observed experimentally.

The studs used for these tests were selected on the basis of rigidity and ease of installation rather than structural modeling. The studs\* were approximately 1/8 inches long and 1/8 inches in diameter with a formed head 1/32 inches long by 3/16 inches in diameter. These particular studs were originally intended for an automotive application. A preliminary evaluation indicated that they provided adequate rigidity. Their real attraction was the availability of a semi-automatic stud welding gun (the square array specimen alone required approximately 1200 studs).

All shells were wrapped around plywood forms cut to a 30 inch diameter ( $\pm 0.005$  inches) and held with steel bands during spot welding of the lap seam. Foil resistance strain gages were then applied opposite to the seam and an oil coating applied to the shell to prevent bonding of the concrete. Copper-constantan thermocouples were attached to the shell and buried in the reinforced concrete. Strains were measured and recorded before and during the placement of the concrete. After the stabilizing sand slurry was removed the inside surface of the liner was finished with a black high temperature paint to enhance radiation.

A micrometer barrel and extension rod were placed in the concrete near the strain gages. This device was used to provide a controlled perturbation by advancing the micrometer inward while the shell was heated. The strain levels at which the shell would not return to the unperturbed state and the calculated minimum post buckling strains are presented in Table 1. Photographs of each of the 10 inch long specimens are shown in Figures 15 through 18. All of the photographs show signs of plastic deformation of the liners since the material had a relatively low yield (45,000 psi) and the temperature was allowed to climb after buckling had occurred. The unsupported liner, Figure 15, had a single plastic hinge at the crest of the buckle wave. The "ring mode model", Figure 16, had three plastic hinges as suggested by Young and Tate [17]. The "ring supported model", Figure 17, buckled in a lobar mode [21]. The "square array model", Figure 18, exhibited both ring mode and single panel buckling modes.

Adequate correlation was obtained for square array stud patterns while the unsupported shell enjoyed no correlation\*\*. Many reasons can be advanced for the lack of correlation between the experimental and analytical results. Some of these reasons are summarized as follows:

- 1.) It is experimentally difficult to cause buckling of the liner at the minimum post buckling strain.
- 2.) The perturbation device provided a point disturbance for all specimens rather than disturbance simulating the buckle mode.
- 3.) All shells experienced plastic deformation while the analytical model was based on an elastic material.
- 4.) The unsupported shell and the shell which can form a buckle wave shorter than the stud spacing appear to have a large energy barrier.

\*Supplied by Nelson Stud Welding, Lorain, Ohio.

\*\*The analysis for the unsupported shell did correlate with the analysis and experiments of Chan and McMinn [3,4].

All of these arguments tend to support the correlation between analysis and experiment for the liner anchored with a square array of studs. Additional data and information on the testing technique can be found in Reference [25].

#### Ring Models

In an effort to obtain experimental data on the effects of stud flexibility on the buckling behavior of liners as well as stud and liner loads after buckling, a series of "beam models" were fabricated and tested. A sketch of the test specimens and the testing configuration can be found in Figure 19. These specimens were designed to be approximately 1/3 scale model slices of cylindrical elements with a Corten steel liner of 0.114 inches and stud anchors 3/8"D x 4" long. The test specimens were 8 inches wide with three studs centered across the width on 3 inch centers. These dimensions were selected so that reasonable scaling of the anchor-concrete behavior could be expected.

Three specimen configurations were examined for each of three testing schemes. The variations of specimen configuration involved only a change of stud spacing along the length of the beam. Stud spacings of 8, 5-3/8 and 4 inches were selected to force buckling elastically, at yield and plastically, respectively. Three initially flat specimens were loaded mechanically in four point bending as shown in Figure 19 so that the gage section was subjected to a state of pure bending with the liner on the compression side. Three beams cast to an initial curvature of 20 feet were tested in the same manner. Finally, three flat specimens were locked in the four point load fixture and subjected to a temperature increase on the liner side with quartz lamps glow bars. The mechanical loading fixture was used to constrain the specimens during the thermal test to prevent relaxation of the thermally induced strains due to gross elastic deflection of the composite beam.

Each specimen was instrumented with foil strain gages on the liner and studs and copper constantan thermocouples on the liner, studs and in the concrete. Gages were placed on opposite sides of the liner plate at the midspan and adjacent to the stud anchors. Gages were applied to the liner in the panel adjacent to panel expected to buckle in an effort to measure the relaxation of this panel after buckling. Opposing gages were placed on the studs adjacent to panel expected to buckle, to provide tensile and bending data on the stud prior to and following buckling. Finally an LVDT displacement transducer was used to obtain center point displacement of the beam so that the precise radius of the liner at the instant of buckling could be recorded. The results of these tests are presented in Table 2. Photographs of the buckled specimens are shown in Figures 20 through 23.

As in the case of the rigid stud supported liner shell, the experimentally observed buckling strain is substantially greater than the minimum post buckling strain which suggests the existence of a large energy barrier isolating the post buckled region. The ring models also exhibited plastic deformation as a result of buckling with plastic hinges at the crest of the buckle wave and at the studs as suggested by Young and Tate [17].

The flexible stud analysis assumed a linear behavior for each of the modes of stud deformation. Two alternate sets of stud stiffnesses were analyzed and interesting results obtained. First the tensile and flexural deformations of the stud are essentially independent of the stiffnesses examined. As a result, the tensile and flexural stud load are directly related to the assumed stud stiffnesses. The shear loads carried by the studs after buckling are essentially independent of the assumed shear stiffness, with the tangential displacements of the studs inversely proportional to the shear stiffnesses. These two

observations are supported by the realization that the tensile and flexural loads in the studs arise by their influence in altering the length of the detached region of the liner while the shear load is produced by the membrane relaxation of the unbuckled portion of the shell. These observations greatly simplify the solution of studs for anchoring liner shells.

The stud stiffnesses used for this study were:

$$k_T = 3.52 \times 10^6 \text{ lbs/in} \quad k_s = 3.25 \times 10^7 \text{ lbs/in} \quad \text{and} \quad k_b = 11.15 \times 10^7 \text{ in-lb/radian.}$$

The minimum post buckling strains for a liner with  $R/t = 2000$  and flexible studs at  $0.0333$  radian was calculated to be approximately  $1240\mu \text{ in/in}$ . The results presented in reference [23] for rigid studs was approximately  $1250\mu \text{ in/in}$ . These stiffnesses were multiplied by  $0.1$  and a new minimum post buckling strain found to be approximately  $1230\mu \text{ in/in}$ . This suggests that the minimum post buckling strain is essentially independent of the assumed stud stiffnesses.

Design charts for specifying cylindrical liner shells and stud anchors were under preparation at the time of writing of this paper. They will be presented subsequently in reference [29].

#### REFERENCES

- [1] Lo, Bogdanoff, J. L., Goldberg, J. E., and Crawford, R. E., "A Buckling Problem of a Circular Ring," Proc. 4th U.S. Nat'l. Cong. of Applied Mechanics, Vol 1, 1962, pp. 691-5
- [2] Tsien, H. S., "A Theory for the Buckling of Thin Shells," J. Aero Sci., Vol. 9, 1942 pp. 373-384.
- [3] Chan, H. C., and McMinn, S. J., "The Stability of a Uniformly Compressed Ring Surrounded by a Rigid Circular Surface," Int. J. of Mech. Sci., Vol. 8, 1966, pp. 433-442.
- [4] Chan, H. C., and McMinn, S. J., "The Stabilization of the Steel Liner of a Prestressed Concrete Pressure Vessel," Nuclear Engineering and Design, Vol. 3, 1966, pp. 66-73.
- [5] Hsu, P. T., Elkon, J., and Pian, T. H. H., "Note on the Instability of Circular Rings Confined to a Rigid Boundary," J. Appl. Mech., Vol. 31, No. 3, Series E, pp. 559-562, Sept 1964.
- [6] Bucciarelli, L. L., Jr., and Pian, T. H. H., "Effects of Imperfections in the Instability of a Ring Confined in an Imperfect Rigid Boundary," J. Appl. Mech., Paper No. 67-APM-U.
- [7] Zagustin, E. A., and Herrmann, G., "Stability of an Elastic Ring in a Rigid Cavity," J. Appl. Mech. Vol. 34, Series E, No. 2, June 1967, pp. 263-270.
- [8] Pian, T. H. H., and Bucciarelli, L. L., Jr., "Buckling of a Radially Constrained Circular Ring Under Distributed Loading," Int. J. of Solids & Struc., Vol 3, pp. 715-30, 1967.
- [9] Chicurel, R., "Shring Buckling of Thin Circular Rings", Trans ASME, J. Appl. Mech. (brief note) vol. 35, Series E, No. 3, September 1968.
- [10] Burgess, I. W., "The Buckling of a Radially Constrained Imperfect Circular Ring," Int. J. Mech. Sci., Vol. 13, pp. 741-753, 1971.
- [11] El-Bayoumy, L., "Buckling of a Circular Elastic Ring Confined to a Uniformly Contracting Circular Boundary," Trans ASME, J. Appl. Mech., Vol. 39, Series E, No. 3, pp. 759-766, September 1973.
- [12] Allan, T., "One-Way Buckling of a Compressed Strip Under Lateral Loading," J. Mech. Engrg. Sci., Vol. 10, No. 2, 1968.

- [13] Allan, T., "One-Way Buckling of Elastically Restrained Columns," J. Mech. Engrg. Sci., Vol. 11, No. 3, 1969.
- [14] Anderson, W. F., "Buckling of a Strip on a Rigid Half-Space with a Transverse Pressure: Wrinkling of a Non-Bonded Cladding," First Int. Conf. on Structural Mechanics in Reactor Technology, Paper C2/6, Sept. 1971.
- [15] Buckhard, A., and Young, W., "Buckling of a Simply-Supported Beam Between Two Unattached Elastic Foundations", AIAA Journal, (Technical Notes) Vol. 11, No. 3, pp. 406-408, 1973.
- [16] Hardingham, R. P., Parker, J. V., and Spruce, T. W., "Liner Design and Development for the Oldbury Vessels," Conf. on Prestressed Concrete Pressure Vessels, The Institution of Civil Engineers, London, 1968, Group J, Paper 56.
- [17] Young, A. G., and Tate, L. A., "Design of Liners for Reactor Vessels," Conf. on Prestressed Concrete Pressure Vessels, The Institution of Civil Engineers, London, 1968, Group j, Paper 57.
- [18] Chapman, J. C., and Carter, "Interaction Between a Pressure Vessel and its Liner," Conf. on Prestressed Concrete Pressure Vessels, The Institution of Civil Engineers, London, 1968, Group J, Paper 58.
- [19] Bishop, R. F., Horseman, R. W., and White, C. M., "Liner Design and Construction," Conf. on Prestressed Concrete Pressure Vessels, The Institution of Civil Engineers, London, 1968, Group J, Paper 59.
- [20] Doyle, J. M., and Chu, S. L., "Liner Plate Buckling and Behavior of Stud and Rib Type Anchors," First Int. Conf. on Structural Mechanics in Reactor Technology, Paper H6/3, Sept. 1971.
- [21] Kiesling, E. W., DeHart, R. C., and Jain, R. K., "Testing of Ring-Stiffened Cylindrical Shells Encased in Concrete - Instrumentation and Procedures," Experimental Mechanics, Vol. 10, No. 6, pp. 251-256, June 1970.
- [22] Kiesling, E. W., DeHart, R. C., Jain, R. K. and Griffith, A. R., "Stability of Ring-Stiffened Cylinder Shells Encased in Concrete," Southwest Research Institute Report, May 1969.
- [23] Kicher, T. P., "Buckling of a Stud Supported Thin Cylindrical Liner Shell Encased in Concrete", Nelson Stud Welding Report, August 1969 and Nuclear Engineering and Design, 1973.
- [24] Tong, P., and Pian, T. H. H., "Buckling of Radially Constrained Thin Spherical Shell Under Edge Load," AIAA 6th Aerospace Sciences Meeting, New York, 1968, paper no. 68-106.
- [25] Esselman, T. C., "Buckling of a Point Supported Liner Shell Inside a Concrete Containment", Ph.D. Thesis, Case Western Reserve University, June 1973.
- [26] Gratzinger, R. J., "Buckling of a Thin Cylindrical Liner Shell Supported in Concrete with Flexible Stud Type Anchors", M.S. Thesis, Case Western Reserve University, June 1973.
- [27] Von Karman, T., and Tsien, H. S., "The Buckling of Thin Cylindrical Shells Under Axial Compression," J. Aero. Sci., Vol. 8, June 1941, pp. 303-312.
- [28] Tsien, H. S., "Lower Buckling Load in the Nonlinear Buckling Theory for Thin Shells," Q. J. Appl. Math., Vol. 5, 1947, pp. 236-237-
- [29] Kicher, T. P., "Design Charts for Cylindrical Liner Shells and Stud Anchors," Report in Preparation.

Table 1  
Analytical and Experimental Results for Complete Shell Models  
(strain units -  $\mu$  in/in)

<u>Stud Configuration</u>	<u><math>\epsilon_0^*, \beta</math></u>	<u><math>\epsilon_{min}</math></u>
Unsupported	-580,-0.33**	-200
5/8" axially by 2-1/4" circumferentially	-1020,0.3	-700
2-1/4" axially by 5/8" axially	-1475,0.47	--
7/8" x 7/8"	-1591,1.0	-1430

\* Total Strain induced in the liner by the curing of the concrete and confined thermal expansion.

\*\*Negative  $\beta$  indicates free axial expansion.

Table 2  
Experimental Results on "Beam Specimens"  
(strain units -  $\mu$  in/in)

<u>Stud Spacing</u>	<u>(R) Buckle</u>	<u>Linear Strain Buckling</u>	<u><math>\epsilon_s</math> Stud Strains at Buckling</u>	<u>Minimum Post Buckling Strain</u>	<u>Predicted Stud Strain at <math>\epsilon_{min}</math></u>
Mechanical Loading of Flat Specimens					
7" - Elastic*	180 inches	-1200	100 $\pm$	-1400	374 $\pm$ 50
5-3/8"-at Yield	173 inches	-4475	800 $\pm$ 400	-2150	172 $\pm$ 55
4" - Plastic	114 inches	-8650	187 $\pm$ 112	-3750	215 $\pm$ 130
Mechanical Loading of Curved Specimens					
8" - Elastic	180 inches	-2450	100 $\pm$ 150	-1150	570 $\pm$ 47
5-3/8"-at Yield	173 inches	-3700	235 $\pm$ 10	-2150	172 $\pm$ 55
4" - Plastic	114 inches	-9400	350 $\pm$ 50	-3750	215 $\pm$ 130
Thermal Loading of Flat Specimens					
8" - Elastic	flat	-1700	100 $\pm$ 200	-1150	570 $\pm$ 47
5-3/8"-at Yield	flat	-3350	200 $\pm$ 600	-2150	172 $\pm$ 55
4" - Plastic	flat	-4000	266 $\pm$ 250	-3750	215 $\pm$ 130

\*A seven inch spacing used for this single preliminary specimen.

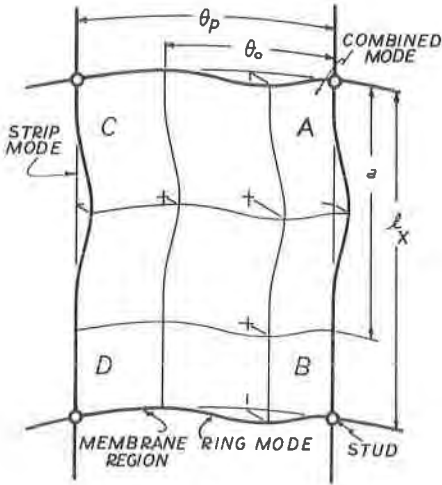


Figure 1. Assumed Displacement Pattern for Cylindrical Elements Supported by Rigid Studs.

	$0 < \theta_0/\theta_p < 1$	$\theta_0/\theta_p = 1$
Pure Membrane	Ring Mode and Membrane Segment Between Studs	Ring Mode Only Between Studs
Strip Mode and Membrane Segment Between Studs	Incomplete Ring and Strip Modes Over Region Between Studs (See Figure 1)	Complete Ring Mode and Incomplete Strip Mode Between Studs
Strip Only Between Studs	Incomplete Ring Mode and Complete Strip Mode Between Studs	Intersecting Modes Over Entire Region

Figure 2. Various Types of Buckling Modes Identified by the Extent of Propagation of the Detached Liner  $\theta_0/\theta_p$  and  $a/l_x$ .

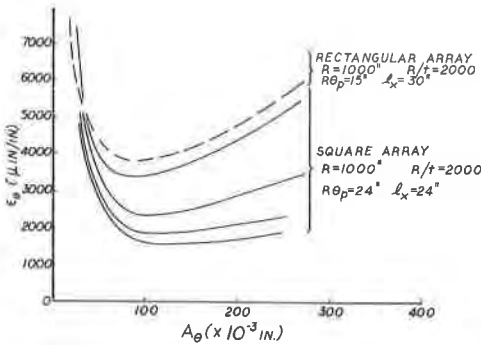


Figure 3. Post Buckling Curves for Square and Rectangular Stud Patterns.

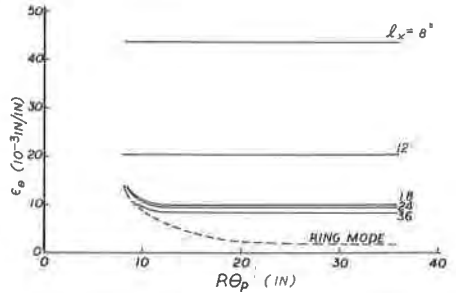


Figure 4. Minimum Post Buckling Strains for Various Stud Configurations,  $R/t = 2000$ ,  $R = 1000$ ,  $\beta = 0$ .

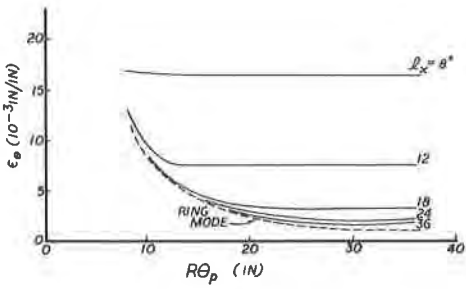


Figure 5. Minimum Post Buckling Strains for Various Stud Configurations,  $R/t = 2000$ ,  $R = 1000$ ,  $\beta = 0.5$ .

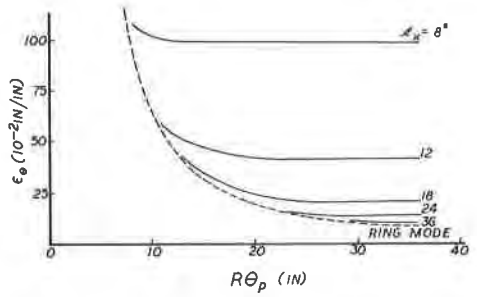


Figure 6. Minimum Post Buckling Strains for Various Stud Configurations,  $R/t = 2000$ ,  $R = 1000$ ,  $\beta = 1.0$

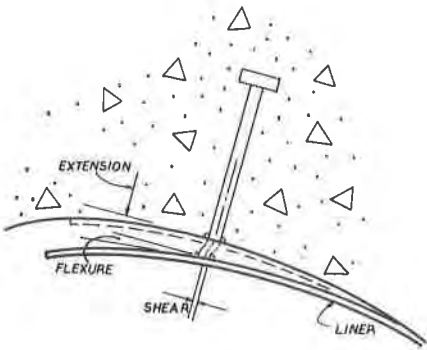


Figure 7. Extension, Shear and Flexure Deformation of an Elastic Stud Support for a Liner Shell.

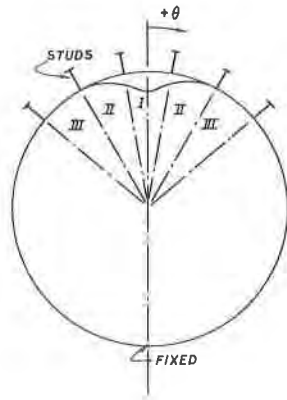


Figure 8. Propagation of Buckle Pattern Introduced by Elastic Studs.

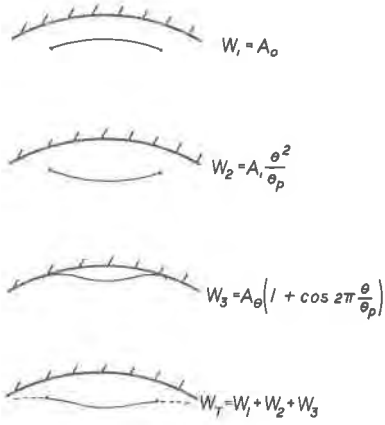


Figure 9. Terms of the Assumed Displacement Pattern.

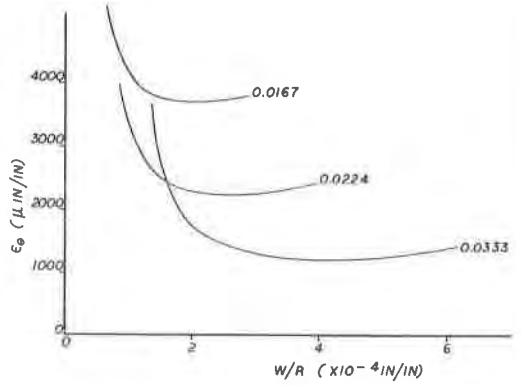


Figure 10. Post Buckling Curves for Elastic Stud Supported Ring With  $R/t = 2000$ . The Stud Spacings are Shown in Radians.

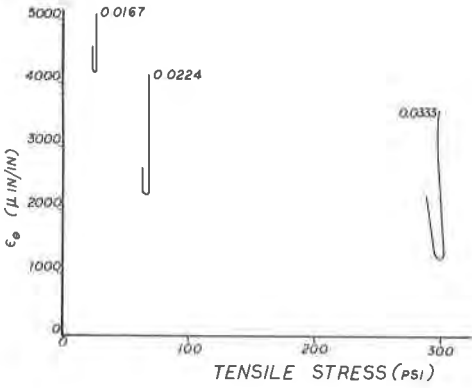


Figure 11. Stud Tensile Stresses vs. Circumferential Liner Strain.

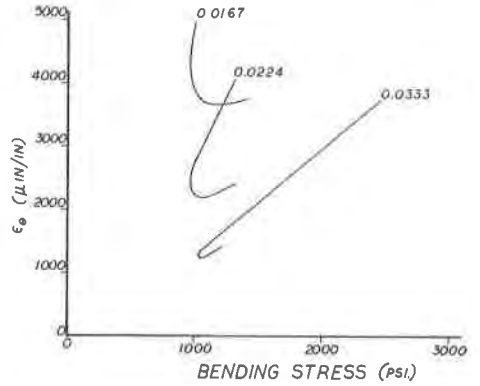


Figure 12. Stud Bending Stresses vs. Circumferential Liner Strain

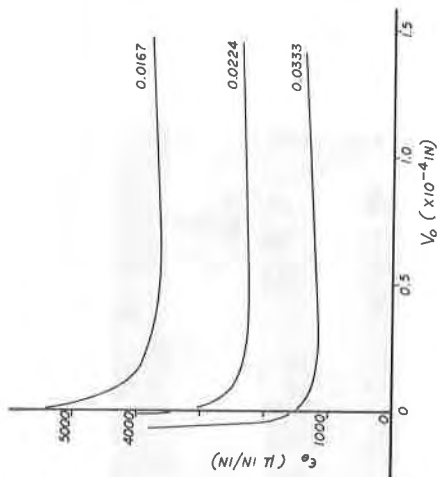


Figure 13. Shear Displacement at Stud Adjacent to Primary Buckle Wave ( $\theta = \theta^0$  P/2).

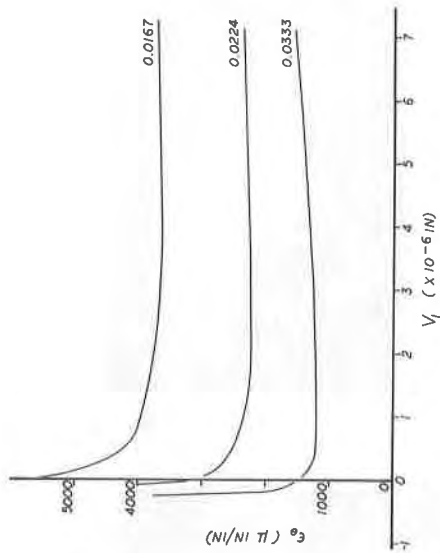


Figure 14. Shear Displacement at Second Stud ( $\theta = 3\theta^0$  P/2).



Figure 15. Unsupported Liner Shell Specimen.



Figure 16. "Ring Mode Model" Liner Shell Specimen.



Figure 17. "Strip Mode Model" Liner Shell Specimen. (Lobar Mode)

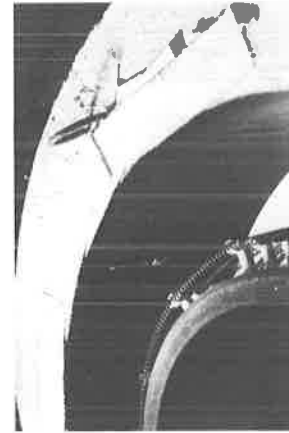


Figure 18. "Combined Mode Model" Liner Shell Specimen.

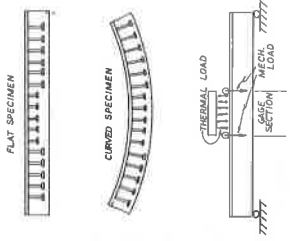


Figure 19. Ring Models and Test Configuration.

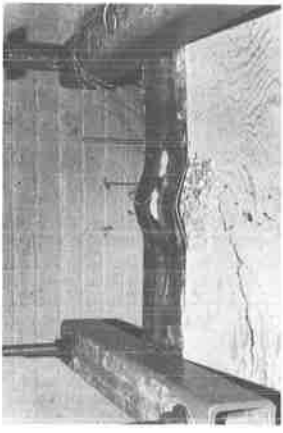


Figure 20. Mechanical Loading of Initially Flat Specimen with Studs on 7" Centers. Note Fracture of Concrete.

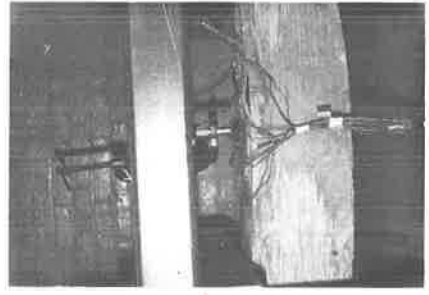


Figure 22. Mechanical Loading of Initially Curved Specimen with Studs on 4" Centers.

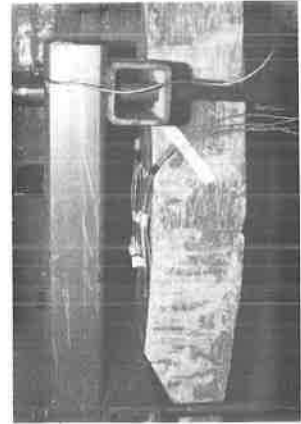


Figure 21. Mechanical Loading of Initially Curved Specimen with Studs on 8" Centers.

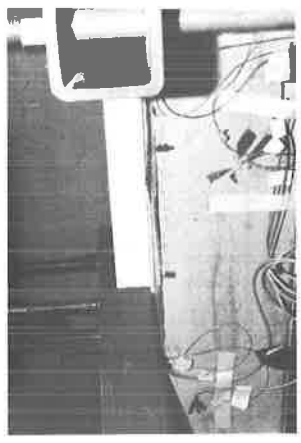


Figure 23. Thermal Loading of Initially Flat Specimen with Studs on 8" Centers.